ELSEVIER

Contents lists available at ScienceDirect

Automation in Construction

journal homepage: www.elsevier.com/locate/autcon



Unmanned rolling compaction system for rockfill materials

Qinglong Zhang^a, Tianyun Liu^a, Zhaosheng Zhang^b, Zehua Huangfu^b, Qingbin Li^{a,*}, Zaizhan An^a



- ^a State Key Laboratory of Hydroscience and Engineering, Tsinghua University, Beijing 100084, China
- ^b Qianping Reservoir Construction and Management Administration, Zhengzhou 450003, China

ARTICLE INFO

Keywords:
Compaction parameters
Compaction quality control
Unmanned rolling compaction system
Real-time remote monitoring
Farth-rock dams

ABSTRACT

The compaction quality of earth–rock dams is mainly controlled by compaction parameters (the number of compaction passes, compaction trajectory, vibration frequency, lift thickness, and driving speed) during construction. However, relying on the operator to implement control of the compaction parameters can result in unrolled, cross-rolling, and repeated-rolling problems between adjacent work faces. Additionally, existing compaction quality control methods cannot satisfy the requirements of construction operations under all weather and extreme conditions. This paper presents an unmanned rolling compaction system for rockfill materials during construction, including an in situ unmanned roller that is based on automatic driving technology, a real-time kinematic global positioning satellite system, a wireless communication system, and a real-time remote monitoring centre based on the client/server mode. The control effect and advantages of the proposed system were proven by a case study on the Qianping Project in China. Consequently, it was demonstrated that the proposed system is considerably automatic, accurate, efficient, and reliable for avoiding the influence of human factors and, ultimately, improving the compaction quality and efficiency of earth–rock dams.

1. Introduction

Compaction is the process by which the volume of rockfill materials is reduced to increase its density. An effective compaction quality control is crucial for the safe and stable operation of earth-rock dams [1,2]. According to existing specifications for earth-rock dam construction, compaction quality mainly depends on the manual control of compaction parameters (the number of compaction passes, compaction trajectory, vibration frequency, lift thickness, and driving speed) during construction and random spot tests after construction [3]. However, there are problems associated with conventional compaction quality control methods: 1) the control of compaction parameters is performed by on-site construction personnel and, thus, is classified under the empirical control method, which results in more control errors and quality defects; 2) spot tests with their destructive characteristics are time-consuming and labourious and, therefore, cannot satisfy the requirements of modern mechanised construction; and 3) the compaction quality of the entire rolling construction cannot be recorded in real time, and data traceability is extremely deficient. Thus, conventional control methods not only fail to effectively control the compaction quality of the construction area but also cannot satisfy earth-rock dam construction quality control requirements, which are becoming increasingly stringent.

Real-time monitoring systems of rolling compaction construction parameters, including continuous compaction control (CCC) [4,5], roller-integrated compaction monitoring (RICM) [6,7], and intelligent compaction (IC) systems [8,9] have been studied in the past to improve compaction quality and efficiency. The CCC system is a data acquisition system that was installed on the compaction equipment to continuously collect real-time information pertaining to the operation and performance of the compactor [4,10,11]. Since the introduction of CCC technology, several studies have been performed to relate roller-measured values to various location-specific measurements (such as density, modulus, penetration resistance, and the California bearing ratio), and thus control the compaction quality of soil [11–18].

Roller-integrated compaction monitoring technology is comprised of internal sensors that are installed on the roller to monitor vibration information, such as harmonic frequencies and accelerations, to determine the RICM measurement value (RICMMV) for characterising the real-time compaction status of compacted materials (subgrade soils, granular soils, and asphalt) [7,19–21]. An on-board computer, with a rugged display screen [22] and a global positioning satellite (GPS) system to map the spatial location of the roller, are also installed as part of the monitoring technology [17]. As a compaction quality control tool for earth materials, the RICM offers tremendous potential for ensuring investments and construction quality and promoting construction

E-mail address: qingbinli@mail.tsinghua.edu.cn (Q. Li).

^{*} Corresponding author.

progress [7]. Recent efforts in the United States and in Europe have focused attention on how RICM technologies can be used in road building [10,23-26], as well as how its parameters can be related to mechanistic pavement design values [7]. Several manufacturers currently offer RICM technologies on smooth drum vibratory roller configurations to monitor the compaction quality of granular materials and asphalt, as well as non-vibratory configurations for monitoring the compaction quality of cohesive materials. These manufacturers define different RICMMVs to characterise the real-time compaction quality of soil, aggregates, and hot mix asphalt (HMA), such as the compaction metre value (CMV) used by Geodynamic [27,28], ks used by Ammann [29], machine drive power (MDP) used by Caterpillar [19,22,30], and OMEGA used by Bomag [31]. To realise these expectations and to accelerate the implementation of RICM, detailed and statistically robust field studies are needed to improve the understanding of relationships between machine parameters (i.e., RICMMV) and various in situ compaction measurements [27]. Therefore, White et al. [27] conducted a field study with 30-m test strips using five granular materials to evaluate CMV and MDP roller-integrated compaction technologies. In addition, Zhong et al. [32] utilised RICM technology to realise the precise automatic online entire-process monitoring of compaction parameters, including the number of compaction passes, compaction trajectory, driving speed, vibration status, and lift thickness. This proposed method provides a new approach for construction quality control of high core rockfill dams. Based on Zhong's research and the RICM technology, Liu et al. [2] collected the real-time field operation data of the driving speed, the number of compaction passes, vibration status, and lift thickness of gravel-mixed cohesive soil at the core wall zone of an earth-rock dam, as well as the corresponding moisture content and gradation of dam materials to control compaction quality during earth-rock dam construction. To overcome the deficiencies of CV (proposed by Liu et al. [20]) and CMV [27,28] in characterising the compaction quality of rockfill materials, Zhang et al. [33] first proposed the roller-integrated acoustic wave detection technique to determine the compaction quality of rockfill materials.

When the RICM system provides automatic feedback control for vibration amplitude/vibration frequency, or driving speed, it is referred to as intelligent compaction (IC) technology [7]. The IC technology has been implemented in Europe and in Japan for years and was introduced to the USA in the late 2000s [29,34,35]. Currently, IC technology is used mainly for quality control and quality assurance of road materials, including HMA [36–45], soils [46–49], and aggregates [48,49]. Simultaneously, intelligent construction systems based on the IC technology have been studied in the past to improve efficiency and safety, including intelligent navigation strategies [50], autonomous systems with artificial intelligence approaches [51], and instrumented roller compactor system monitoring vibration behaviour [52]. Other intelligent systems that have been studied for the asphalt paving industry include those that use neural network modelling [36,53] and an onboard density reading system [36,45].

However, because the earth-rock dam construction technology and its quality control standards differ from those of road construction, the technologies mentioned above are not appropriate for controlling the compaction quality of earth-rock dams. Even though several scholars have attempted to apply the abovementioned techniques to earth-rock dams, evident problems have remained unresolved: 1) manual driving will lead to control error, and the operator will significantly influence the control effect of compaction parameters, thus resulting in inferior compaction uniformity; 2) during the rolling construction of the connection strip between two adjacent sections, there are unrolled, crossrolling and repeated-rolling problems; 3) the abovementioned technologies cannot satisfy the ever-increasing demands for compaction quality and efficiency in dangerous areas, all weather, and extreme conditions; 4) the compaction efficiency of the earth-rock dam is critically affected by human factors. To solve the foregoing problems, as well as deficiencies in traditional compaction quality control methods,

some researchers have attempted to utilise automatic driving technology (ADT) to achieve rolling operations. With the advent of automatic navigation and driving technology, the above problems and deficiencies are expected to be resolved. In agriculture, Luo et al. [54] developed an automatic navigation and control system based on the real-time kinematic (RTK)-GPS technology, which has been used to solve the farmland bottleneck problem of crooked sowing. In addition, Wei et al. [55] developed an automatic navigation and steering system for transplanters to have automatic alignment and head steering functions. However, automatic navigation and driving techniques have not vet been applied to earth-rock dam construction. Therefore, by referencing previous research, this paper proposes an unmanned rolling compaction (URC) method and system for rockfill materials in earthrock dam construction. The developed system can effectively control compaction parameters and significantly improve deficiencies of existing compaction quality control methods, avoid compaction defects, and subsequently improve compaction quality and efficiency.

2. Related works

In recent years, researchers have actively adopted real-time monitoring systems of rolling compaction construction parameters in monitoring compaction parameters. As the basis of these systems, the accuracy of GPS measurement is directly related to the monitoring effect of the compaction parameters, and the compaction parameters are closely related to the compaction quality of the filling materials [3]. Therefore, GPS has been widely used in the monitoring of compaction parameters and construction quality. Liu et al. [20] utilised RICM technology based on RTK-GPS to monitor the number of compaction passes, compaction trajectory, driving speed, and vibration status in earth-rock dam construction. Xu and Chang [38] evaluated the effectiveness of IC technology based on RTK-GPS for asphalt compaction, and the results show that the IC roller equipped with the RTK-GPS system can maintain a continuous record of the number of compaction passes, locations of the roller, driving speed and vibration frequency. Kassem et al. [56] developed a compaction monitoring system based on the latest GPS technologies to monitor the compaction of asphalt pavement, and the colour-coded maps based on the GPS reflected the number of passes, the location of the compaction roller, and other indexes. Anderegg et al. [57] used CCC technology based on the differential GPS system to provide the roller operator with a simple visual aid to show him the compaction that was attained, the number of compaction passes and other data of the construction site.

In addition, GPS-combined interpolation and grid partition has been used in several research studies to determine lift thickness. A fairly simple approach involved obtaining the elevation (Z-value) measurements from the RTK-GPS on a CCC compactor for one lift and comparing those values to the elevation measurements from the previous lift, thereby determining the lift thickness by the difference between two elevation measurements at the same location [58]. The CCC equipment never records data at the same two locations in space (the same X and Y coordinates) from lift to lift. To bypass this problem, a fixed-position (X, Y) coordinate grid and the RTK-GPS measured elevation values for a given lift, as well as geospatial interpolation methods, were utilised to predict the corresponding elevations at each of the grid points, and then when the elevation at each of the gird points has been determined for the two neighbouring lifts, the lift thickness at each grid point location can be calculated by taking the difference in elevation from the successive layer [59]. In addition, the ordinary Kriging method is used for the spatial interpolation of roller measured values (MV) of elevation to predict unknown values on a uniform grid for each lift of the constructed embankment and to determine lift thickness [60]. An alternative interpolation approach for predicting elevation values at each of the grid point locations is the inverse distance weighting (IDW) method, and the final compacted thickness of each soil lift can be determined by comparing the interpolated elevation

value at each grid point location with the interpolated value at the same grid point location for the underlying lift [60,61].

Some roller manufacturers and third-party companies, such as Ammann [57], Geodynamik [28], Caterpillar [62], Bomag [8], and Trimble [6], have also developed corresponding CCC/RICM/IC devices that are integrated with GPS to monitor the compaction parameters during construction. GPS-based compaction equipment manufactured by Ammann was used to monitor the number of compaction passes, and a combined DGPS/laser system was capable of achieving height precision in millimetres, thereby determining the lift thickness in combination with three-dimensional digital coordinate grid technology [63]. IC equipment with an RTK-GPS system made by Caterpillar was provided. and it was utilised to monitor the thickness of compacted soil lifts during the construction of a roadway embankment, and both simple and sophisticated spatial analysis techniques were used to interpolate measured field elevation data onto a uniform grid for a lift thickness assessment [60,64]. The Trimble intelligent compaction system with on-board high-precision GPS was used to continuously monitor the number of compaction passes, the compaction trajectory and lift thickness of the railway subgrade [65]. Our previous work [33,66,67] realised a RTK-GPS based, real-time compaction quality detection and automatic driving utilised in earth-rock dam construction. The abovementioned studies served as the backdrop for the research described in this paper to adopt RTK-GPS and uniform grid technologies, as well as a number of supporting technologies, to monitor the compaction parameters (driving speed, the number of compaction passes, vibration status, and compaction trajectory) and to determine the lift thickness.

3. Unmanned rolling compaction system

In previous studies [66,67], the authors proposed a concept of ADT for hydraulic engineering and developed an automatic driving vibratory roller. In this study, the authors further developed the URC system to control the compaction quality of rockfill materials in earth–rock dams. The framework of the URC system is shown in Fig. 1. The system consists of the unmanned roller, the RTK-GPS system, the wireless communication system, and the remote monitoring centre. The unmanned roller collects its own status information in real time, feeds it back to the remote monitoring centre, receives the navigation line sent

by the centre to achieve automatic navigation and driving, and receives control commands to achieve remote control driving. The remote monitoring centre formulates the navigation line, receives various status information and emergency request information fed back by the unmanned roller in real time, and sends real-time control instructions to the unmanned roller. Moreover, the remote monitoring centre can achieve comprehensive monitoring of the compaction parameters. The RTK-GPS system includes an RTK-GPS base station and moving station, which were used to obtain the current position coordinates of the vibratory roller. Specifically, the base station receives GPS satellite signals and determines the phase difference of the transmitted carrier in real time, and the moving station determines the high precision position of the vibratory roller based on the GPS signals it received, and phase difference signals of the carrier were transmitted by the base station. The wireless communication system provides service not only for communication between slow-moving construction equipment but also for the transmission of remote control and on-site monitoring information.

The proposed URC system has several advantages. First, it realises the unmanned operation of the rolling process based on ADT and accurately controls the compaction parameters (the number of compaction passes, driving speed, vibration frequency, compaction trajectory, and lift thickness), thereby effectively improving the compaction quality of earth-rock dam materials during the rolling process. Second, the system continuously monitors the entire rolling process and enables timely feedback for quality control. Third, it frees people from complicated operations and reduces the impact of human factors on the compaction quality. Fourth, it can satisfy the requirements of on-site all-weather and high-strength filling construction. Fifth, it can effectively solve the unrolled, cross-rolling, and repeated-rolling problems that exist between adjacent work faces. Finally, the abovementioned advantages improve the compaction quality and efficiency of rockfill materials in earth-rock dams, which can enhance the overall project performance.

3.1. Unmanned roller

The unmanned roller mainly includes on-board navigation controller with a built-in navigation control program (NCP), GPS receiver

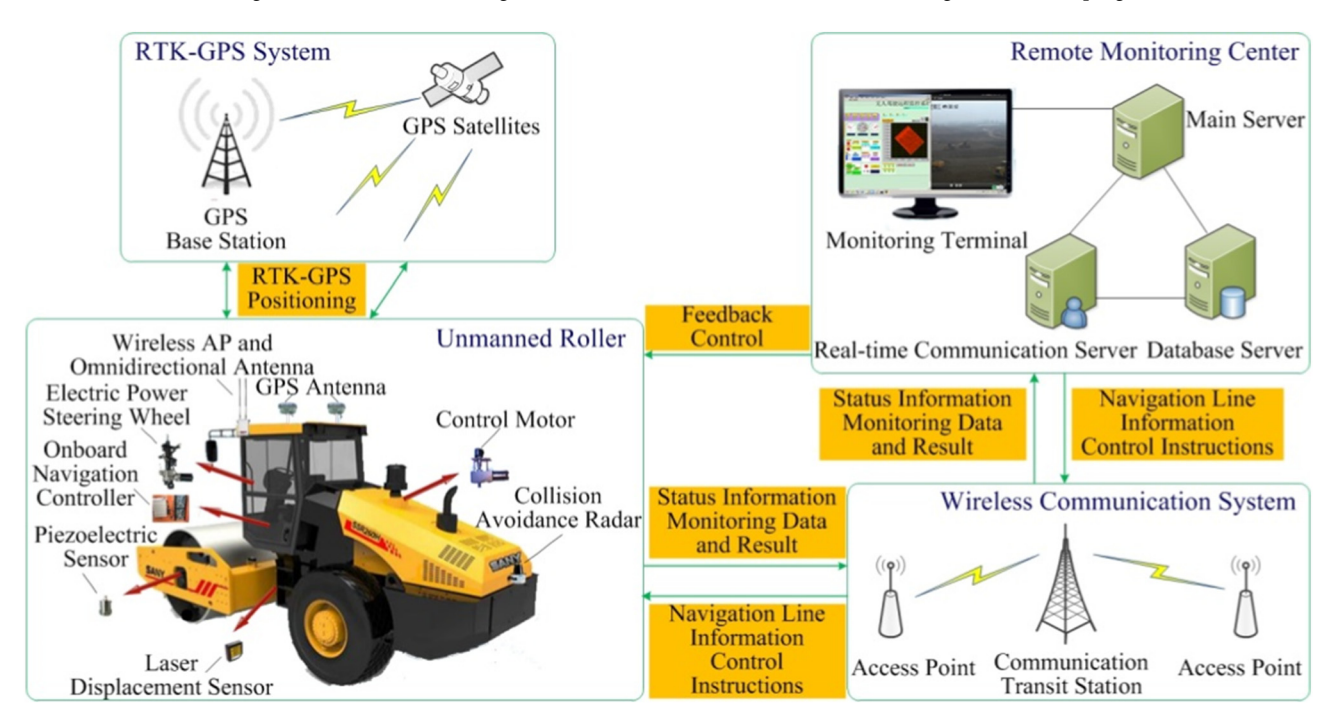


Fig. 1. Framework of the URC system.

and antennas, wireless access point (AP), wireless AP omnidirectional, inter-vehicle communicator, ground speed radar, collision avoidance radar, control motor, electric power steering wheel, and piezoelectric sensor (Fig. 1). As the key to an embedded system, the NCP is responsible for receiving and sending control information, as well as receiving commands and inputting target amount sent by the remote monitoring centre in real time. In addition, it receives RTK-GPS position data, ground speed radar data, ranging radar data, and steering angle sensor data in real time.

The NCP first executes a remotely controlled instruction for powering, starting, or shutting-off the vibratory roller. Thereafter, the NCP calls the steering control subroutine, compares the deviation of the navigation target input amount and the positioning data, and determines the desired steering angle; NCP compares the difference between the desired steering angle and the actual steering angle of the wheel and automatically controls the steering wheel according to the output current of the PID algorithm. As a result, the vibratory roller is rotated in a predetermined direction. In addition, the NCP also calls the automatic acceleration subroutine to compare the expected travel speed input values, ground speed radar measurement speed, and automatic brake operating conditions; and to control the automatic throttle actuator through the output current control of the PID algorithm according to the status of nearby vehicles, thereby driving the vibratory roller at the desired speed.

Additionally, the NCP also invokes an automatic brake subroutine to compare the degree of range-variations of obstacles in the ranging radar, to determine the movement of other nearby vehicles through inter-vehicle communication, and to control the brake pedal based on the output current control of the PID algorithm, thereby slowing down or stopping the vibratory roller. Thereafter, the NCP sends information, such as vibration status, position information, driving speed, automatic control status, and environmental video to the remote monitoring centre in real time. Additionally, the on-board navigation controller actively detects the distance between nearby vehicles and properly adjusts the throttle and brake based on a pre-defined safe distance and speed. As a result, it achieves an automatic driving function that has been adapted to the surrounding conditions.

3.1.1. On-board automatic control system

The flowchart of the on-board automatic control system is shown in Fig. 2. After the on-board navigation controller is started, the NCP first performs an initialisation process. Thereafter, the NCP establishes a connection with the remote control device through wireless communication, establishes the RTK-GPS connection, and initialises the navigation control cycle, PID parameters, and other related state parameters. Afterwards, the NCP starts to detect the working status of each sensor and actuator of the entire automatic control system. If any component fails to work properly, then the NCP will record its status parameters and send relevant information to the remote monitoring centre, where it will wait for related problems to be handled; otherwise, the NCP will not perform automatic navigation operations. If the NCP passes the self-test of the system, then it will enter the automatic navigation operation, which is divided into a series of automatic navigation processes according to the navigation control cycle. For each process, there are three sub-processes: automatic steering control, automatic speed regulation, and automatic brake.

a. The automatic steering control sub-process first reads the navigation target value and navigation direction, and, thereafter, reads the latitude and longitude coordinates of its current position and converts it into plane coordinates. Second, automatic steering control calculates the distance between the current position and navigation direction, which is the horizontal deviation value and converts the lateral deviation value into the desired automatic steering expectation angle in the current control cycle according to the current speed. Third, automatic steering control reads the current steering

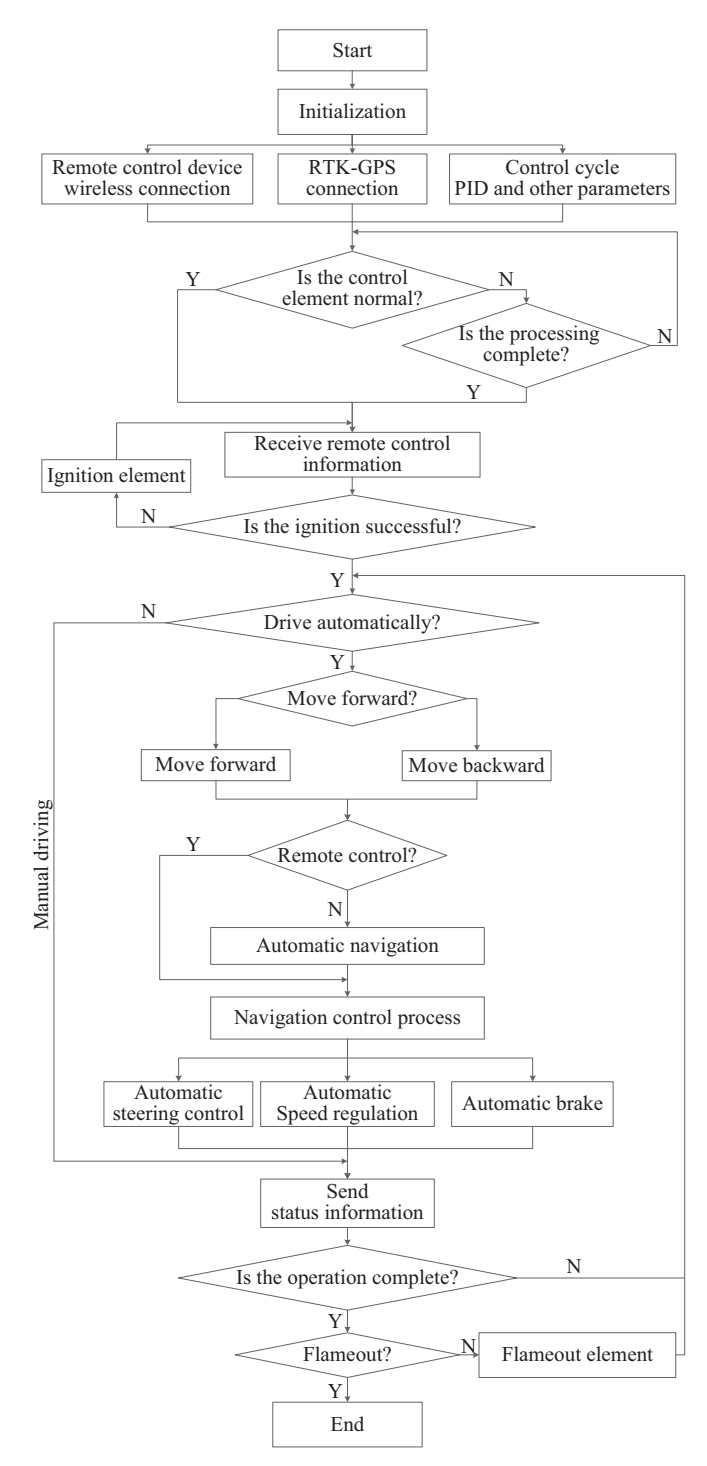


Fig. 2. Flowchart of on-board automatic control system.

angle of the steering wheel angle sensor and determines whether the current steering angle has reached the limit that was set by the system or is less than the desired automatic steering angle. It is only when the current steering angle is less than the limit value that the steering PID control subroutine is invoked. After the PID control subroutine compares the current steering angle with the expected automatic steering angle, the PID adjustment is performed for the rotation angle deviation. Thereafter, the control current signal is calculated and transmitted to the electric steering wheel to realise the automatic steering of the roller, thereby completing one cycle of the automatic steering control process.

b. The automatic speed regulation sub-process first reads the expected

input value of the navigation speed and collision avoidance radar signal. It then reads the ground speed radar measurement value of the roller to ascertain whether the driving speed reaches the speed limit value that was set by the system. If the driving speed is less than the limit, then the PID control subroutine for speed adjustment is invoked. After comparing the current speed value and the expected input speed value, the PID control subroutine adjusts the speed deviation, calculates the control current signal to the electric throttle device, and adjusts the driving speed of the vibratory roller, thereby completing the automatic speed regulation process in one cycle.

c. The automatic brake sub-process is classified into three types of brake situations; parking, work, and emergency. For the parking situation at the end of the navigation work, the sub-process first reads the coordinates of the navigation target position. Then, it reads the position coordinate data that were obtained by the RTK-GPS. After it compares the navigation target position with the current position, according to whether the position deviation is within the system error range, it determines whether the current brake signal is to be transmitted to the electric brake device to achieve brake and parking tasks. For acceleration and deceleration work brake conditions, when the throttle device is in the closed-valve state, the PID brake subroutine is called according to the distanceshortening change speed difference between the roller and the obstacle. The PID program adjusts and controls the brake current signal and transmits it to the electric brake device, thereby achieving the purpose of the driving speed adjustment. For an emergency brake situation, when a stop signal is unexpectedly received, the maximum current signal is directly output to the brake device to achieve a rapid stop, thereby completing a cycle of the automatic driving brake process.

3.1.2. Three-dimensional navigation map

In path planning and navigation, a reasonable data model first needs to be established. The model uses the object-oriented concept and method to abstract spatial points and roads into node and unit classes to master the whole process of the model and manage each class separately.

The design principles of the three-dimensional (3D) navigation map data model should satisfy a simple graphical structure, small redundancy, simple topological relationship, fast spatial information query, and open data interface. The flowchart of the data model is shown in Fig. 3 below:

- a. Read in the map file. The map file must satisfy certain format requirements, including the output optimal path filename, road network model type, domain type, number of nodes, number of units, number of sections, space coordinates of each node, node number contained in each unit, and section information.
- b. Create a road network model. According to the read map file, the domain, node, unit, and section information are saved in corresponding classes, such as the Domain class, DofManager class, Element class, and CrossSection class.
- c. Form an overall stiffness matrix. According to the node and element information in the road network model, a one-dimensional overall stiffness matrix with variable bandwidth storage can be formed to provide a basis for path planning.
- d. Solve the optimal path. According to the node connection information provided in the one-dimensional global stiffness matrix with variable bandwidth storage, the Dijkstra algorithm is used to

solve the shortest path problem in directed graphs; the A* algorithm is used to solve the shortest path in a static road network, and the D* algorithm is used to solve the shortest path in a dynamic environment, which can determine the optimal path for both overall and local path planning for obstacle avoidance.

3.1.3. Overall path planning

The algorithms Dijkstra, A^* , and D^* can each be used for overall path planning. Of the three, Dijkstra is extremely classical but is not heuristic and requires a large amount of calculation. However, A^* and D^* have better intelligence and can quickly identify the optimal path. Moreover, D^* is a dynamic algorithm that can re-plan the optimal path when road conditions change.

To determine the more appropriate algorithm for overall path planning, this study adopts the same type of complex road network model (path.in) to verify the accuracy and computational efficiency of Dijkstra, A*, and D*. The road network model (path.in) has a total of 2500 nodes and 9702 cells. Each internal node is connected to 8 nodes surrounding it, and the interval between the horizontal and vertical nodes is 1. Based on the road network model (path.in), this study utilises the three algorithms to calculate optimal distances of paths that have various starting and ending points, namely, 1-2500, 2-2500, 50-2451, and 100-2451. The results from obtaining these optimal paths and the elapsed time used to solve them are summarised in Table 1. Based on the list in Table 1, A* and D* significantly improved the computational efficiency compared to that of Dijkstra. Moreover, because D* has the advantage of being able to re-plan the path if road conditions change, this study ultimately selects the D* algorithm to realise the overall path planning for the URC system.

3.1.4. Obstacle avoidance in local path planning

Section 3.1.3 indicates that the D* algorithm has more advantages in the overall path planning. When the roller encounters obstacles during the movement process, the D* algorithm utilises the last planned information to search for the route again, avoids duplicate calculation of the same data, and improves the efficiency of secondary planning. However, the D* algorithm also has a few drawbacks. Because the roller will inevitably be involved in cornering as it moves, D* searches in four or eight directions around the current position each time it turns a corner. Moreover, being a length-first algorithm, the resulting path will have several unnecessary turns. When the D* algorithm searches for a path, it first locates obstacles before re-searching for other adjacent shortest feasible paths. Consequently, the generated path will stick with the obstacle and may even encounter two adjacent obstacles. In view of the above problems and based on previous research [67,68], this study has selected the improved D* algorithm based on the CA model as the obstacle avoidance local path planning algorithm to ensure that the roller will move in an effective path, with no collision, at a low cost.

3.2. RTK-GPS system

The RTK-GPS system is a position and navigation system that is based on real-time kinematic technology and can achieve a centimetre-level positioning accuracy. This system has been used in several studies for real-time data acquisition, real-time construction machinery positioning, and navigation at the construction site. Su et al. [69] proposed an enhanced boundary condition method to control the accuracy of the construction location system integrated with the RTK-GPS system and RFID. Robert et al. [70] utilised the RTK-GPS technology to aid construction plants in dynamic control and autonomous guidance. Liu et al.

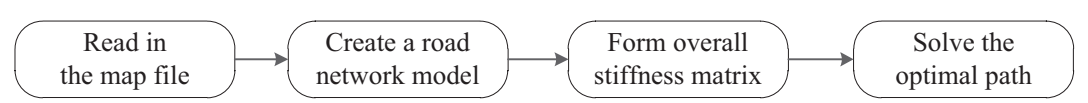


Fig. 3. Flowchart of the 3D navigation map data model.

Table 1
Time utilised by the three algorithms for the path.in model and the optimal path calculation.

Algorithm	Time (s)				Optimal path (m)			
	1–2500	2–2500	50-2451	100–2451	1–2500	2–2500	50-2451	100–2451
Dijkstra	0.257	0.247	0.257	0.245	69.30	68.88	69.30	68.88
A*	0.087	0.091	0.088	0.090	69.30	68.88	69.30	68.88
D*	0.090	0.093	0.085	0.089	69.30	68.88	69.30	68.88

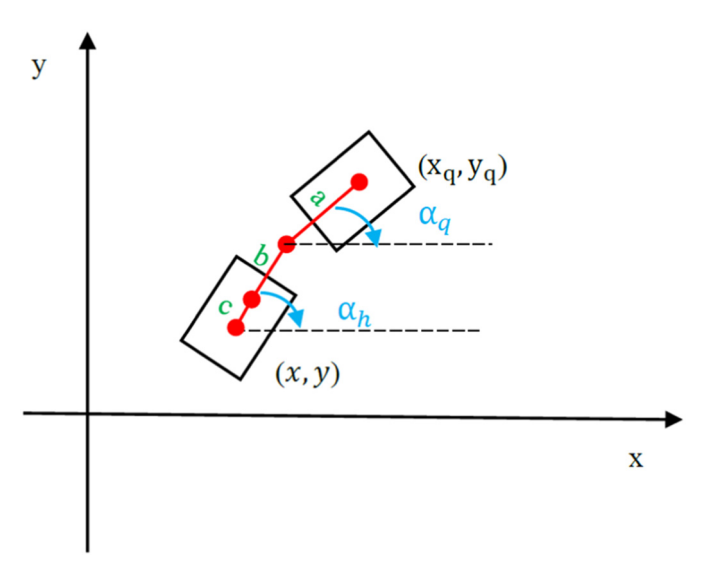


Fig. 4. Schematic of the vehicle body composition.

[20] used it to achieve real-time spatial viewing of CVs and compaction quality, as well as to visually indicate locations of quality defects. In addition, our previous research [33] proposed using the roller-integrated acoustic wave detection technique for rockfill materials based on RTK-GPS technology. According to the abovementioned studies, this study has selected RTK-GPS technology to realise the high-precision positioning and navigation functions of the URC system.

The RTK principle is that the GPS mobile station not only receives information from the base station but also receives information that is transmitted by satellite. Thereafter, it performs differential processing on two types of coordinate information to obtain high-precision data. After obtaining the optimal path between two points on the road

network, autonomous navigation can be performed by using the ADT. The core of the automatic driving navigation is to use the coordinate information that was provided by the RTK-GPS to calculate the distance deviation, e_1 , and angular deviation, e_2 , between the vehicle body and the optimal path in real time to calculate the steering angle and achieve automatic driving. The specific processes of navigation are as follows:

- (1) Convert the GPS latitude and longitude information into construction coordinates by coordinate conversion;
- (2) Calculate the rear body azimuth, α_h , based on the left and right GPS coordinates:
- (3) Use the controller area network communication to obtain the actual steering angle, α_f , of the steering wheel, and thereby acquire the azimuth, α_q ($\alpha_q = \alpha_h + \alpha_f$), of the front body;
- (4) Calculate the coordinates (x_q, y_q) of the front or rear wheel centre in combination with the GPS and azimuth;
- (5) Calculate the distance deviation, e_1 , and angular deviation, e_2 , between the vehicle body and the navigation route;
- (6) Calculate the steering angle, $t\alpha_f$, based on deviations e_1 and e_2 , and thereby achieve automatic driving navigation.

3.2.1. Coordinate transformation

By setting the GPS mobile station through the TestSerial software, data that include only the GPGGA statement can be transmitted every 0.1 s. After parsing the longitude and latitude information in the GPGGA, the geodetic coordinates can be obtained by Gaussian projection. Thereafter, four-parameter (x_0, y_0, R_1, R_2) transformation can convert the geodetic coordinates into local coordinates through the following conversion formula:

$$\begin{bmatrix} x \\ y \end{bmatrix} = \begin{bmatrix} x_0 \\ y_0 \end{bmatrix} + \begin{bmatrix} R_2 & R_1 \\ -R_1 & R_2 \end{bmatrix} \times \begin{bmatrix} x' \\ y' \end{bmatrix}$$
 (1)

where x and y are coordinates of the target coordinate system, x' and y'

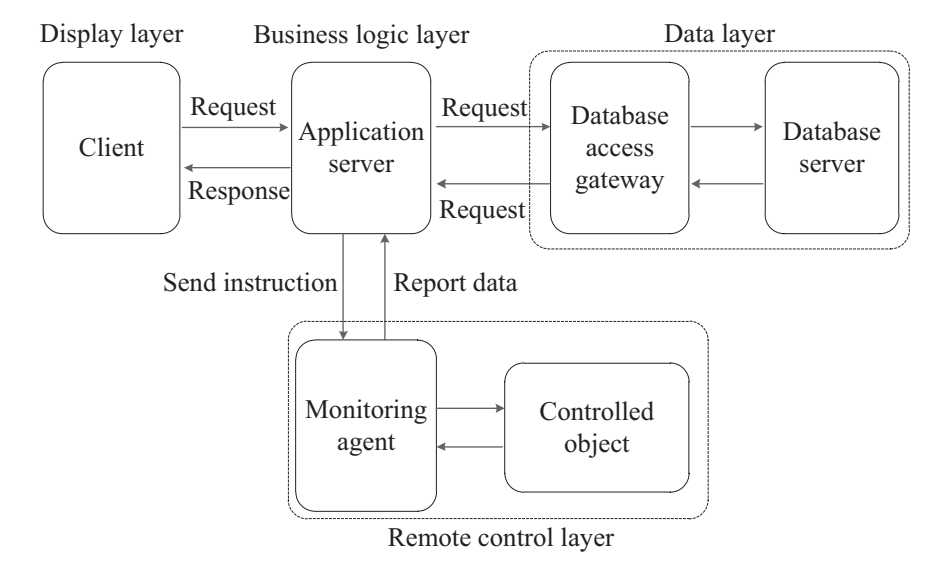


Fig. 5. Schematic diagram of remote monitoring centre.

Server

Wireless

transmission

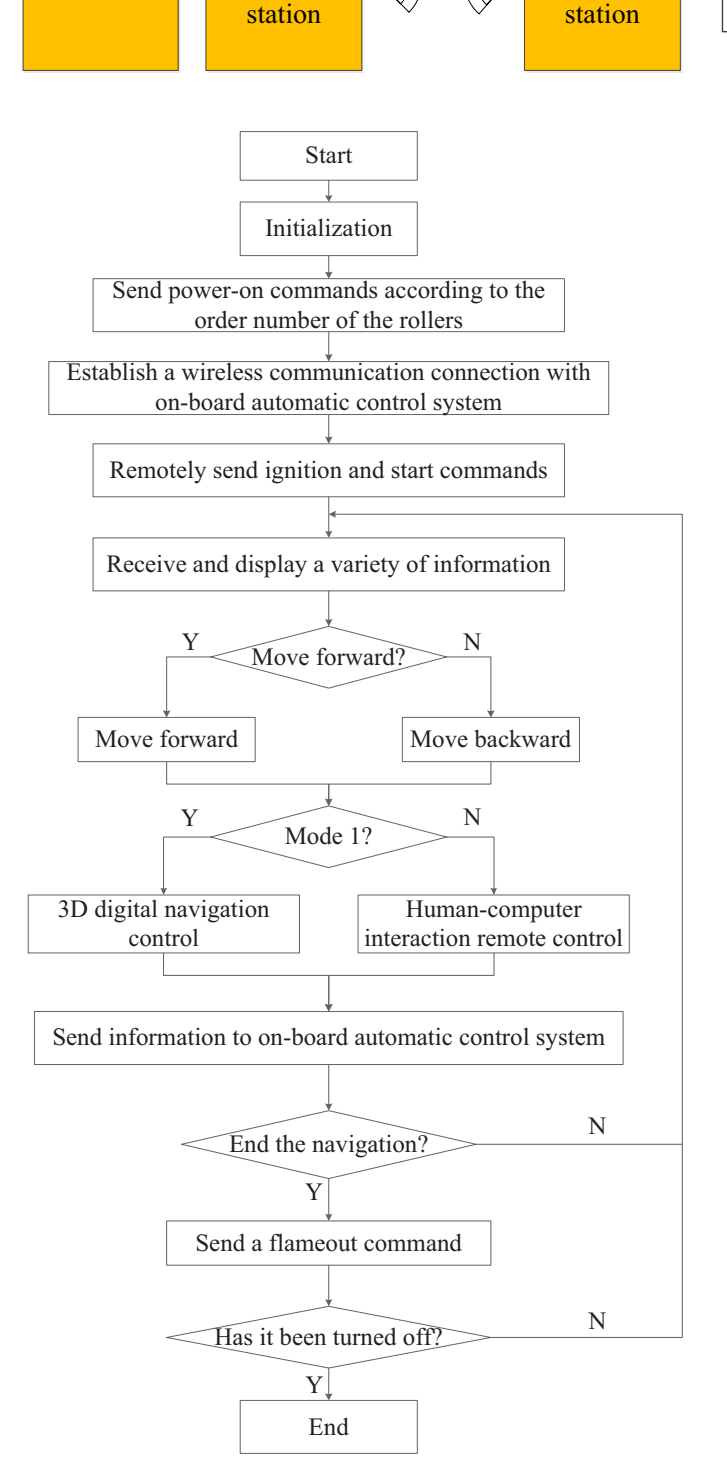


Fig. 7. Flowchart of the remote monitoring system for the roller.

are coordinates of the source coordinate system, x_0 and y_0 are translation parameters, and R_1 and R_2 are rotation parameters.

3.2.2. Vehicle body azimuth

The rear body azimuth, α_h can be calculated according to the coordinates of the left and right sides of the GPS rover; the calculation formula is shown in Eq. (2). The front body azimuth can be calculated

Fig. 6. Schematic of the real-time video surveillance system.

from the rear body azimuth, as well as the actual steering angle of the steering wheel using Eq. (3).

$$\alpha_h = \arcsin\left(\frac{|x_1 - x_r|}{\sqrt{(x_1 - x_r)^2 + (y_1 - y_r)^2}}\right)$$
 (2)

$$\alpha_q = \alpha_h + \alpha_f \tag{3}$$

where (x_1, y_1, z_1) and (x_r, y_r, z_r) are coordinates of the left and right sides of the GPS rover, respectively.

3.2.3. Elevation correction formula

Camera

Industrial computer

Wireless

transmission

Because the actual road has a certain slope, the left and right sides of the GPS rover also have specifically high tolerances, which will have particular influence on the coordinates of the centre point between the left and right sides of the GPS rover projected to the horizontal plane. Hence, the elevation should be corrected using the following formulae:

$$EC = \sqrt{(x_1 - x_r)^2 + (y_1 + y_r)^2}$$
 (4)

$$x = \frac{x_1 + x_r}{2} - h \frac{z_1 - z_r}{EC} \sin \alpha_h \tag{5}$$

$$y = \frac{y_1 + y_r}{2} + h \frac{z_1 - z_r}{EC} \cos \alpha_h \tag{6}$$

where EC is the elevation correction, (x_1, y_1, z_1) and (x_r, y_r, z_r) are coordinates of the left and right sides of the GPS rover, respectively; h is the height of the vehicle body; and (x, y) are coordinates of the centre point between the left and right sides of the GPS rover.

3.2.4. Front and rear wheel coordinate formulae

The body composition of the roller is shown in Fig. 4. By obtaining a (the horizontal distance from the centre of the front wheel to the intermediate hinge), b (the horizontal distance from the centre of the rear wheel to the intermediate hinge), and c (the horizontal distance from the centre of the rear wheel to the coordinates of the centre point between the left and right sides of the GPS rover), the coordinates (x_{fq}, y_{fq}) of the front wheel centre or the rear wheel centre can be derived. The front wheel coordinates can be calculated by Eqs. (7) and (8), and the rear wheel coordinates (x_{rq}, y_{rq}) can be calculated by Eqs. (9) and (10).

$$x_{fq} = x + (b + c)\cos\alpha_h + a\cos\alpha_q \tag{7}$$

$$y_{fq} = y + (b + c)\sin\alpha_h + a\sin\alpha_q$$
 (8)

$$x_{rq} = x + c \cdot \cos \alpha_h \tag{9}$$

$$y_{rq} = y + c \cdot \sin \alpha_h \tag{10}$$

3.2.5. Deviation and steering angle

According to the coordinates of the front wheel centre or rear wheel centre, the distance deviation, e_1 , and the angular deviation, e_2 , of the vehicle body from the navigation route can be calculated. Moreover, the steering angle, ta_f , can be calculated in accordance with the actual steering angle, a_f , and deviations e_1 and e_2 of the steering wheel. Furthermore, the steering wheel is controlled in real time because of ta_f ; consequently, the roller travels based on a predetermined trajectory. Consequently, automatic driving is fully realised.



Fig. 8. Photograph of the URC system testing at the rockfill zone.

Table 2
Test scheme for the URC system at the rockfill zone located downstream.

Area	Range	Date	Number of layers	Pile number	Number of compaction passes
A	0 + 200-0 + 400 m	7/11/2017–25/11/ 2017	9	A/B/C/D/E/F/G/H/I	2/8
В	0 + 400-0 + 680 m	23/9/2017–24/11/ 2017	14	a/b/c/d/e/f/g/h/i/j1/j2/k/l/m/n/o/p/q/r/s/t/u/v/w/x/y/z/aa/ bb/cc/dd	2/8

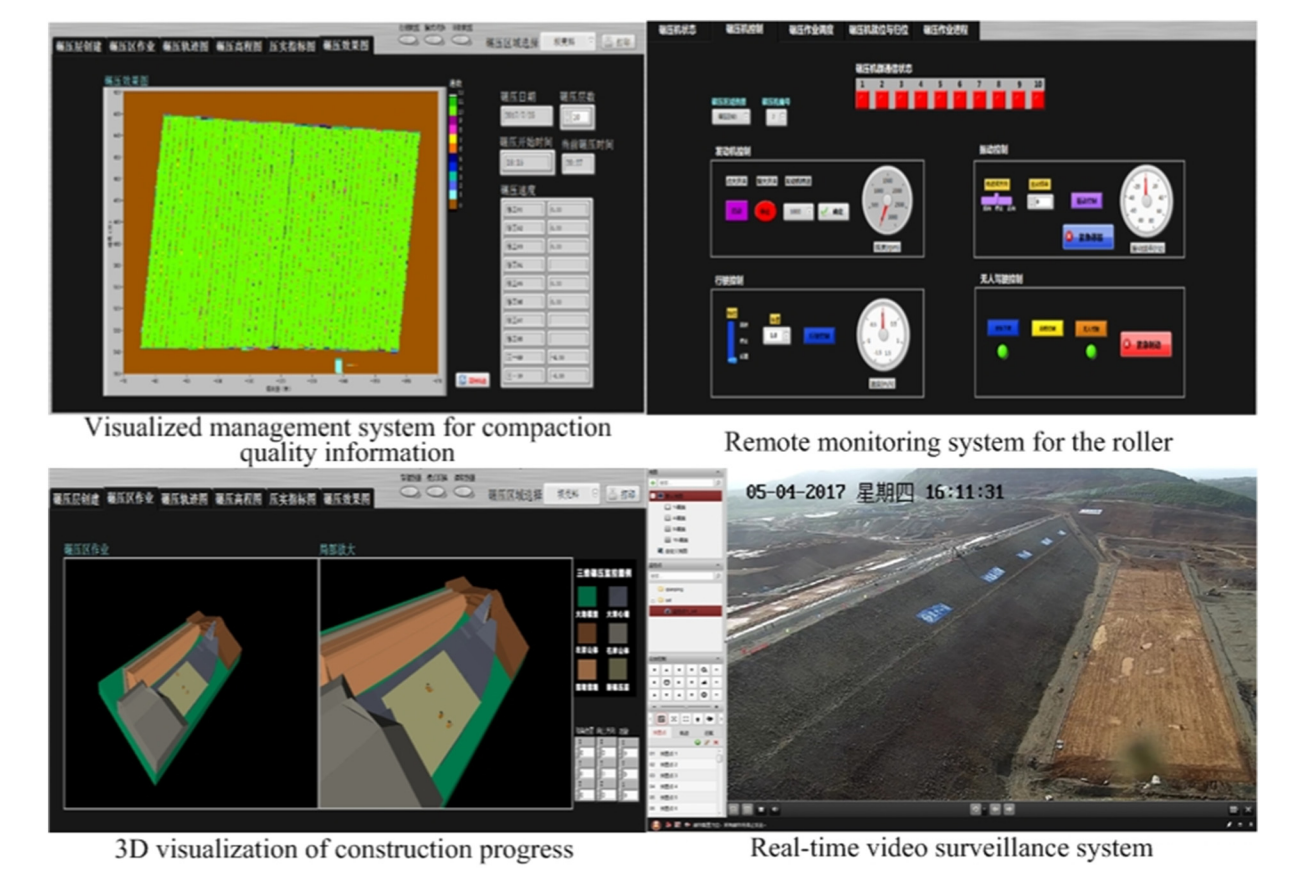


Fig. 9. User interface of the unmanned rolling compaction system for Qianping project.

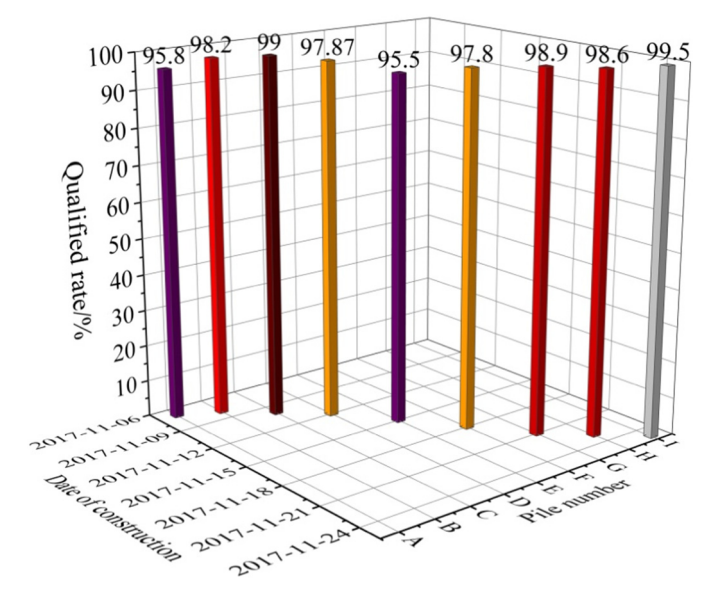


Fig. 10. Qualified rate of the number of compaction passes for area A.

3.3. Wireless communication system

Communication between the remote monitoring centre and the unmanned roller is mainly realised by the wireless communication system; the communication method is a full-duplex serial mode. The wireless communication system (see Fig. 1) consists mainly of the AP located on the roller, the communication transit station, and AP located on the remote monitoring centre. The AP located on the roller is responsible for sending information on compaction parameters (the number of compaction passes, compaction trajectory, vibration frequency, elevation information, and driving speed) during construction, the working environment video image information and status

information (the distance between the roller and obstacle, and the steering angle of the steering wheel) of the roller to the remote monitoring centre. The communication transit station functions to relay the communicated information to achieve long-distance communication. On the other hand, the AP that is located on the remote monitoring centre sends control commands (ignition, switch on, throttle, brake, and flameout), navigation line data, and remote-control commands during emergencies or special situations to the unmanned roller.

3.4. Remote monitoring centre

The remote monitoring centre includes the real-time video surveil-lance (VS) system of the construction site, the remote monitoring system for the roller, and the visualised management system for compaction quality information. Based on the client/server mode, the remote monitoring centre utilises a four-layer architecture for data communication with controlled objects. The remote monitoring centre structure includes the display layer, business logic layer, data layer, and remote-control layer, as shown in Fig. 5. The user accesses the application server through the self-developed monitoring platform client. Because the business logic processing is on the server side and data processing is completed by the database server, the long-distance and local data access can be performed through the wireless network.

3.4.1. Real-time video surveillance system

The real-time video surveillance system of the construction site mainly realises the monitoring of working conditions, such as the material truck, roller, and bulldozer in the entire filling and rolling construction area, as well as the overall condition monitoring of the construction site. This system (see Fig. 6) is mainly composed of the server, industrial computer, camera, and wireless transmission station. The server, with the industrial computer and camera, utilises wireless communication to transmit data. The camera transmits the live real-time image to the server, and the industrial computer feeds information about the working condition, such as the material truck, roller, and

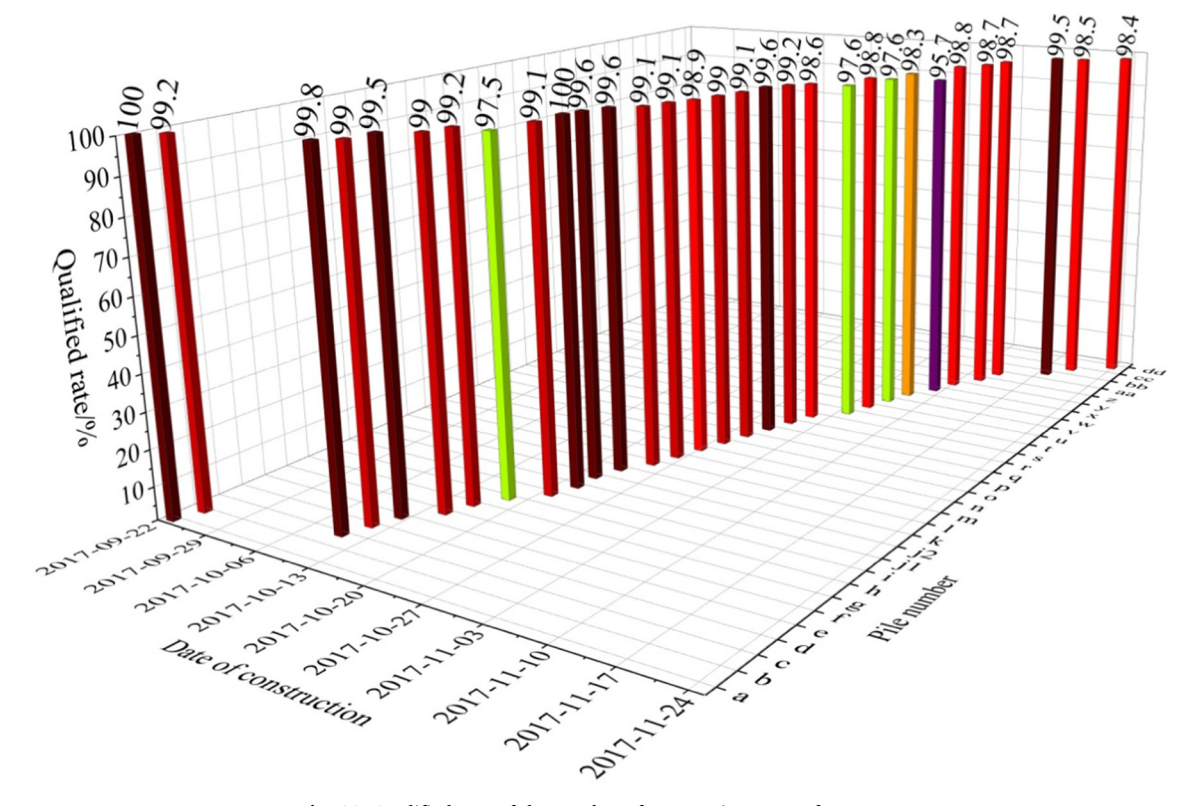
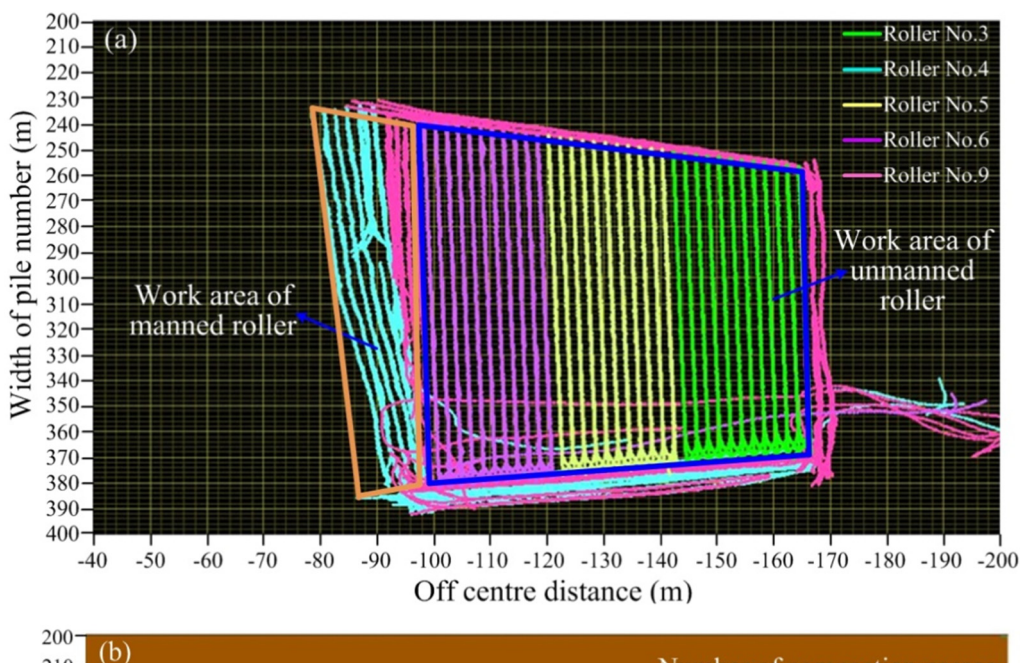


Fig. 11. Qualified rate of the number of compaction passes for area B.



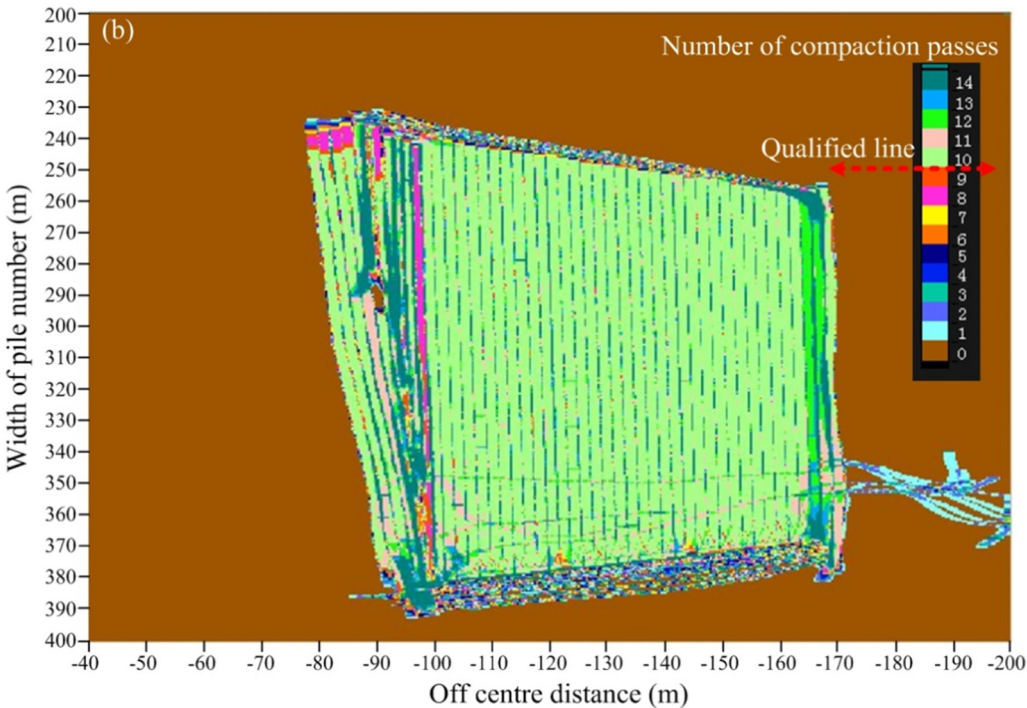


Fig. 12. Compaction parameter monitoring diagram of area A on 15 November 2017: (a) Compaction trajectory; (b) the number of compaction passes.

Table 3Test results of RTK-GPS equipment accuracy.

Coordinate axis	Minimum absolute error/cm	Maximum absolute error/cm	Average absolute error/cm	Minimum relative error/%	Maximum relative error/ %	Average relative error/ %
x	5.34E-08	0.42	0.20	6.65E-8	0.52	0.23
y	7.64E-09	1.94	0.65	2E-8	3.11	1.25
z	1.26	2.97	2.32	3.75	8.91	6.92

bulldozer, to the server in real time.

3.4.2. Remote monitoring system for the roller

The remote monitoring system for the roller mainly includes the control computer and wireless communication antenna. The control computer stores a monitoring program, a 3D digital model of the

construction project, construction schedule program, and navigation planning program. The monitoring program can simultaneously command and control multiple rollers for rolling operations. The flowchart of the remote monitoring system for the roller is shown in Fig. 7. As shown in the figure, after the remote monitoring system for the roller is started, the monitoring program is first initialised to display the status

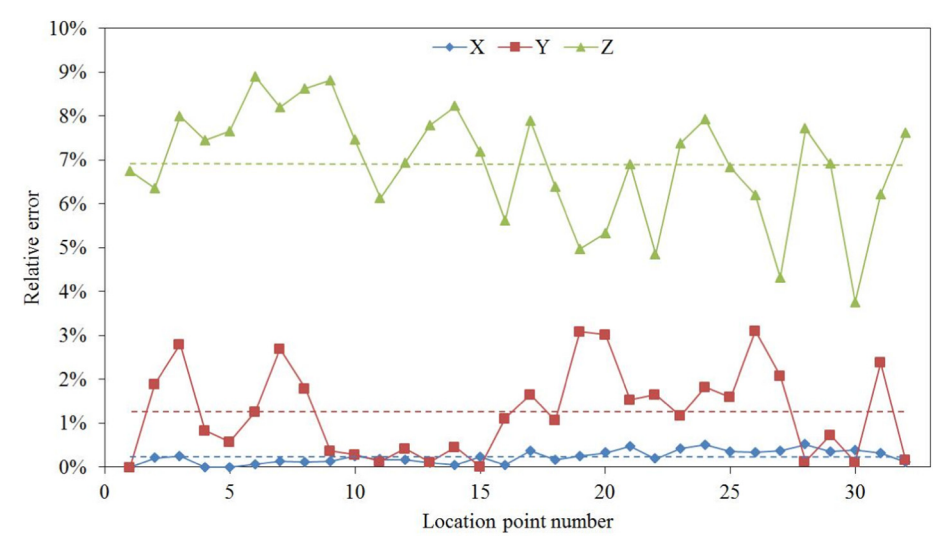


Fig. 13. Relative error of the test results obtained from RTK-GPS and conventional methods.

of the monitoring equipment system and the monitored information status of the rollers; second, the monitoring program successively sends a power-on command remotely according to the order number of the roller; third, the monitoring program establishes a wireless communication connection with the on-board automatic control system of the rollers; fourth, the remote monitoring system receives and displays the video sent by the on-board automatic control system, the spatial position information obtained by RTK-GPS technology, the information on various sensors, as well as the emergency processing request in a specific display frame; fifth, according to the real-time condition of the rollers, the monitoring program remotely sends the ignition and start commands of the rollers; finally, the monitoring program enters the remote 3D digital model navigation control or human-computer interaction remote subroutine.

3.4.3. Visualised management system for compaction quality information

Using AutoCAD, LabView, and other software, this study established a 3D digital model of the earth–rock dam, and then developed a compaction quality information management system based on the client/server mode. In addition, this study introduced the 3D model into the server database, established the data table information based on the rolling time and compaction quality information, realised the compaction quality visualisation of the rockfill materials and the subsequent evaluation function, and then realised the dynamic update of the compaction quality information based on the database file.

4. Case study

4.1. Testing site and materials

The earth–rock dam of Qianping reservoir, with a clay core, is in Henan Province, China. This dam, with a height of 90.3 m, includes six construction zones and four different types of dam filling materials; its gross filling capacity of earthwork is $1.3 \times 10^7 \, \mathrm{m}^3$. This research focused on rockfill materials at major rockfill areas located at the downstream dam body. The rockfill materials at major rockfill areas have a maximum particle size of 1000 mm, based on a conservative estimate, and the proportion of particles less than 5 mm is controlled to within 15%; the average moisture content is 4.8% (based on the average results from 114 groups of tests). For the rockfill materials, the designed standard for the number of compaction is eight.

4.2. Testing program

To analyse the actual effect of the unmanned rolling compaction system that was proposed in this paper, several sets of on-site experiments were implemented. In this study, areas A and B were selected as analysis objects of system operation results. Fig. 8 shows a photograph of the unmanned rolling compaction system test at the downstream rockfill zone, and the experiment scheme is summarised in Table 2. As shown in Fig. 8, areas A and B are located in the rockfill zone at a certain distance from the right dam abutment; several unmanned rollers participated in the entire test plan, such as unmanned rollers 1, 2, and 3.

Vibratory rollers used in this field test consisted of the smooth drum for the rockfill material compaction. According to design requirements, this study conducted 10 compaction operations, which included two static and eight vibration compaction operations (see Table 2) on rockfill materials. During the entire test period, area A was filled with 9 layers, and area B was filled with 14 layers. Because the unmanned rolling compaction system with its corresponding device was employed at the Qianping project, the compaction parameters, frequency of use, and the fault rate of the unmanned roller during the compacting process could be acquired for this project. Fig. 9 shows the user interface of the URC system of this project. We retrieved a set of field-sampling data, including the compaction parameters (the number of compaction passes, compaction trajectory, vibration frequency, lift thickness, and driving speed), use frequency of the unmanned roller, fault rate of the unmanned roller, and the elevation of compacted layers that are used for the actual effect analysis of the unmanned rolling compaction system proposed in this paper.

5. Result analysis

5.1. Result analysis of the compaction parameters

According to the test plan summarised in Table 2, this section presents the statistically analysed results of the compaction trajectory and the number of compaction passes of the filling construction areas A and B. Fig. 10 shows the qualified rate of the number of compaction passes for area A from 7 November 2017 to 25 November 2017, and Fig. 11 shows that for area B from 23 September 2017 to 24 November 2017. Statistical results indicated that when the URC system is used to fill each layer of the two areas, the qualified rates of the number of compaction passes for the filling area having different pile numbers are all above 95%, and most exceeded 98%; the control accuracy of the

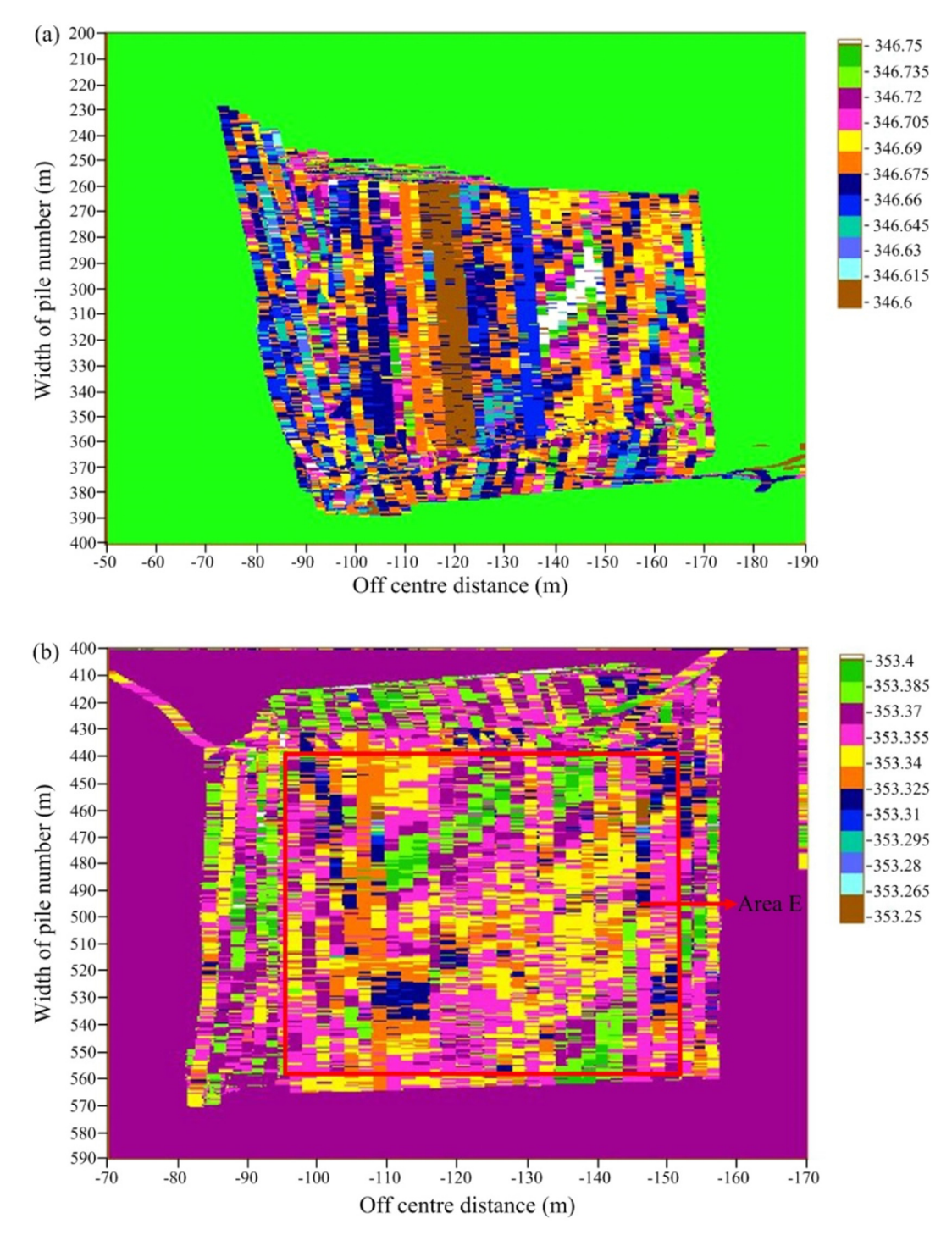


Fig. 14. Elevation information of the work surface after completion of the rolling operations: (a) area A and layer 4; (b) area B and layer 12.

Table 4
Lift thickness and the uncertainty of layer 12 in area E.

Number of grids	Designed thickness/cm	Maximum lift thickness/cm	Minimum lift thickness/cm	Average lift thickness/cm	Uncertainty/cm
3360	80.0	81.0	66.0	75.6	0.04

compaction trajectory is within 5 cm; the control accuracy of vibration frequency and the driving speed are 0.5 Hz and 0.05 m/s, respectively; and the amplitude of the modified roller is consistent with the parameters of the original roller, and can be considered as a constant. The number of compaction passes in some areas may have not satisfied the

standard, because several unmanned rollers are overloaded during the initial operation of the URC system. As a result, any of the following may happen: failure to maintain work schedules, the on-site management of the unmanned rolling area is not in place, a lack of coordination between the management personnel of the remote monitoring

centre and those on site, wireless communication affected by bad weather, or other non-human or non-system factors arise on site.

According to specifications of existing earth-rock dam construction [3], compaction parameters have a significant impact on the compaction quality of earth-rock dams. To visually reflect the control effect of the URC system on the compaction quality, this study selected the compaction parameter monitoring diagram for area A on 15 November 2017 as an example, as shown in Fig. 12. As can be observed from Figs. 10, 11, and 12, the URC system that was proposed in this paper has evident advantages over manual driving. That is, the URC system can accurately control the compaction trajectory, thereby solving the unrolled, cross-rolling, and repeated-rolling problems to effectively ensure the qualified rate of the number of compaction passes: the URC system can accurately control the compaction trajectory, vibration frequency and driving speed, as well as effectively reduce the human influence of the driver on the compaction quality of the rockfill materials; the URC system can achieve real-time visualisation of compaction parameters to realise the whole process under all weather conditions with timely monitoring of the rolling compaction quality; the URC system with the unmanned rolling characteristic is extremely suitable for rolling construction under dangerous conditions, night-time conditions, or extreme conditions (such as in the plateau area). Based on the above analysis, the URC system can effectively control the compaction quality of rockfill materials.

5.2. Statistics and analysis of the use frequency of unmanned rollers

This section describes the use frequency of unmanned and manned rollers during the filling construction of areas A and B, respectively. Statistical results indicate that unmanned rollers are used at a significantly higher frequency than are manned rollers. During the entire test process, unmanned rollers are mainly responsible for the rolling task in the main construction area (see Fig. 12), whereas manned rollers are responsible for the rolling task at the corner and seam (see Fig. 12). Compared with the manned roller, the URC system based on unmanned rollers can perform a crucial function in the filling process of rockfill materials located downstream of the earth–rock dam. Based on the above analysis, the URC system can liberate roller drivers from complicated work, thereby greatly reducing the influence of human factors on compaction quality, and significantly improving the efficiency of filling construction.

5.3. Statistics and analysis of the fault condition of unmanned rollers

This section counted and analysed the fault conditions of unmanned rollers during the rolling construction of areas A and B. Statistical results show that the number of faults of unmanned rollers is significantly less than that of the total, and the result reflects the high reliability of unmanned rollers. Based on statistical analysis, the fault rate of unmanned rollers in areas A and B during construction are approximately 8.8 and 7.9%, respectively. The statistical results indicate that the URC system based on unmanned rollers has characteristics of a stable operation, strong adaptability, convenient maintenance, and remarkable safety.

5.4. Statistics and analysis of lift thickness of compacted layer

5.4.1. Discussion regarding the accuracy of RTK-GPS equipment

Since the construction site is relatively wide and the GPS base station is located on the open platform at the top of the left bank abutment not far from the construction site (see Fig. 8), the communication between the base station and the construction site is not affected by occlusion and trees. This paper selects a set of location points at the test site and verifies the accuracy of the RTK-GPS equipment by comparing it with static GPS and levelling instrument measurement results. A total of 32 sets of test points were used for the accuracy analysis of the RTK-

GPS equipment. Table 3 shows the test results of RTK-GPS equipment accuracy, and the relative error of the test results obtained from RTK-GPS and conventional methods is shown in Fig. 13. From the table, RTK-GPS equipment has a higher accuracy in the plane (x, y) than in elevation (z). The average absolute error of the plane is less than 1 cm, and the average absolute error of the elevation is less than 2.5 cm. As shown in Fig. 13, the average relative error gradually increases from the x direction to the y direction and then to the y direction. The average relative error of the elevation is less than 1.5%, and the average relative error of the elevation is less than 7%. Based on the above analysis, through multiple sets of comparison experiments, the measurement accuracy of the RTK-GPS equipment used in this paper can meet the actual needs of the URC system and in situ construction.

5.4.2. Statistics and analysis of the elevation of the compacted layer

Area A has 9 layers of rockfill materials that were filled from 7 November 2017 to 25 November 2017, whereas area B has 14 layers that were filled from 23 September 2017 to 24 November 2017. Using the monitoring data of areas A and B that were obtained by the URC system, this section reports an evaluation of the elevation data of compacted layers. The results show that the URC system can control the difference between elevations at each position of the compacted layer to within 15 cm (the design standard for the filling layer thickness is 80 cm). The monitoring data of areas A and B on 12 November 2017 are selected as an illustration to better reflect the control effect of elevation, as shown in Fig. 14. Statistical results and Fig. 14 indicate that the URC system can maintain uniform settlement of the compacted layers, thereby controlling the compaction quality of earth–rock dams through the control of lift thickness.

5.4.3. Uncertainty in the computed average lift thickness

To reflect the uncertainty in the computed average lift thickness, area E in Fig. 14 is selected as the calculated test region. Area E is divided into 3360 uniform grids according to a grid size of 2 m by 1 m. After using the URC system for rolling operations according to the specified number of compaction passes, this section statistically analyses the lift thickness data of these grid points. The calculation of the lift thickness, H_k , in grid k is shown through Eq. (11) to Eq. (12) [71]. The lift thickness $h_{k,\ t}$ in grid k at time t is compacted using Eq. (11).

$$h_{k,t} = z_t - Z_{k,0} (11)$$

hence, the lift thickness in the kth gird can be calculated using Eq. (12).

$$H_k = \max_{t} \{h_{k,t}\} = Z_{k,1} - Z_{k,0} \tag{12}$$

 z_t is the elevation at time t, $Z_{k,\ 0}$ is the initial elevation of grid k; and $Z_{k,\ 0}$ is in accordance with the design thickness of the filling layer. The elevation of the gird after compaction is captured in Eq. (13).

$$Z_{k,1} = \max_{t} \{ z_t \mid (x_t, y_t) \in G_k \}$$
 (13)

 $(x_t, y_t) \in G_k$ means that in the *t*th time interval, the trajectory point (x_t, y_t) is in the *k*th gird G_k .

Based on the above formula and type A evaluation method of standard uncertainty, the required lift thickness, maximum lift thickness, minimum lift thickness, average lift thickness, and uncertainty in the computed average lift thickness for the filling layer of area E are presented in Table 4. From Table 4, it can be seen that the measurement results are of high quality, and the lift thickness can be effectively monitored during construction.

6. Conclusion and prospect

The following conclusions were drawn based on the outcomes and findings of this study.

• Based on ADT, RTK-GPS, AP, 3D visualisation, and VS technologies,

an URC method for rockfill materials is proposed. The method with the characteristics of adaptive real-time planning path according to job scene change, two-way high-speed communication, data storage and application separation, automation feedback control, high-precision positioning and navigation, on-board and remote dual control mode, three-dimensional visualisation of the construction process, and monitoring of the whole construction process converts the mode of manned rolling compaction into that of unmanned rolling compaction.

- A real-time URC system for earth-rock dams is developed, and the construction process of the earth-rock dam in the Qianping reservoir project is used as a case study. These data from the monitored construction areas show that the one-time qualified rate of the number of compaction passes is greater than 95%, and most exceeded 98%; the control accuracy of the compaction trajectory is within 5 cm, the control accuracy of the vibration frequency is 0.5 Hz, and the control accuracy of the driving speed is 0.05 m/s. In addition, the statistical results indicate that the URC system can maintain the uniform settlement of compacted layers, thereby effectively controlling the lift thickness. In a word, the compaction parameters are up to standard.
- The field application of this system demonstrated the effectiveness and efficiency of this system. It was found that this system can accurately control compaction parameters; fundamentally solve the unrolled, cross-rolling, and repeated-rolling problems between adjacent work faces; successfully free the operators form tedious work; effectively avoid human errors or extensive management intervention, fully meet the needs of all-weather construction under high-intensity conditions; and continuously monitor the whole process of construction in 3D visualisation. Based on the above conclusions, this system can effectively control the construction process, thereby improving the compaction quality and efficiency of the earth-rock dam, which can effectively improve the performance of the overall project.
- Future research will be conducted in three aspects. First, the control accuracy of the compaction parameters needs to be improved by the optimisation of the software and hardware of the system as well as the control process, an improvement of the system integration, and an in-depth training of the system administrators. Second, the clustering and collaborative operation of multiple unmanned rollers need further study. Third, the URC system can be further extended to RCC dams, railways, highways, airports and dikes, and the related application studies needs to be followed up.

Conflict of interest

The authors declare no conflict of interest.

Acknowledgements

This research was supported by the National Basic Research Program of China (973 Program) (No. 2013CB035902) and the National Natural Science Foundation of China (No. 51339003).

References

- T.B. Hua, X.G. Yang, Q. Yao, H.T. Li, Assessment of real-time compaction quality test indexes for rockfill material based on roller vibratory acceleration analysis, Adv. Mater. Sci. Eng. 2018 (2018) 1–15, https://doi.org/10.1155/2018/2879321.
- [2] D.H. Liu, J. Sun, D.H. Zhong, L.G. Song, Compaction quality control of earth-rock dam construction using real-time field operation data, J. Constr. Eng. Manag. 138 (9) (2012) 1085–1094, https://doi.org/10.1061/(ASCE)CO.1943-7862.0000510.
- [3] D/T5129-2013, Specifications for Rolled Earth-rockfill Dam Construction, China Electric Power Press, Beijing, China, 2013 (ISBN: 155123.1820).
- [4] D. Adam, Continuous compaction control (CCC) with vibratory rollers, Environmental Geotechnics: Proceedings of the 1st Australia-New Zealand Conference on Environmental Geotechnics-Geoenvironment 97, Melbourne, Victoria, Australia, 26–28 November, A. A. Balkema, Rotterdam, (1997), pp.

- 245-250 (ISBN: 90-5410-903-3).
- [5] J. Pistrol, S. Villwock, W. Völker, F. Kopf, D. Adam, Continuous compaction control (CCC) with oscillating rollers, Procedia Eng. 143 (2016) 514–521, https://doi.org/ 10.1016/j.proeng.2016.06.065.
- [6] D.J. White, P.K. Vennapusa, A review of roller-integrated compaction monitoring technologies for earthworks, Final Report ER10-04, Iowa State University, 2010, http://www.intrans.iastate.edu/reports/White%20and%20Vennapusa%202010_ FHWA%20IC%20Lit%20Review.pdf.
- [7] D.J. White, P.K. Vennapusa, H.H. Gieselman, Field assessment and specification review for roller-integrated compaction monitoring technologies, Adv. Civ. Eng. 2011 (2011) 1–15, https://doi.org/10.1155/2011/783836.
- [8] J. Briaud, J. Seo, Intelligent Compaction: Overview and Research Needs, Rep., Texas A&M Univ., College Station, Tex, 2003http://www.intelligentcompaction. com/downloads/PapersReports/Texas_Briaud_IC%20Report_200409.pdf.
- [9] R. Anderegg, K. Kaufmann, Intelligent compaction with vibratory rollers: feedback control systems in automatic compaction and compaction control, Transp. Res. Rec. 1868 (2004) 124–134, https://doi.org/10.3141/1868-13 (Washington, D.C., USA).
- [10] H. Thurner, A. Sandström, A new device for instant compaction control, Proceedings of the International Conference on Compaction, Paris, France, 2 1980 28-5978-019-X, pp. 611–614.
- [11] D. Adam, H. Brandl, Sophisticated roller integrated continuous compaction control, Proceedings of 12th Asian Regional Conference on Soil Mechanics and Geotechnical Engineering-Geotechnical Infrastructure for the New Millennium, Singapore, 2003 98-1238-559-2, pp. 427-430.
- [12] W. Kröber, E.H.R. Floss, W. Wallrath, Dynamic soil stiffness as quality criterion for soil compaction, Geotechnics for Roads, Rail Tracks and Earth Structures, A. A. Balkema Publishers, Lisse, The Netherlands, 90-2651-844-7, 2001, pp. 189–199.
- [13] M.A. Mooney, P.B. Gorman, J.N. Gonzalez, Vibration based health monitoring during earthwork construction, Struct. Health Monit. 2 (4) (2005) 137–152, https://doi.org/10.1177/1475921705049759.
- [14] G. Dondi, C. Sangiorgi, C. Lantieri, Applying geostatistics to continuous compaction control of construction and demolition materials for road embankments, J. Geotech. Geoenviron. 140 (3) (2014) 06013005, https://doi.org/10.1061/(ASCE)GT.1943-5606.0001044.
- [15] D.V. Cacciola, C.L. Meehan, M. Khosravi, An evaluation of specification methodologies for use with continuous compaction control equipment, Proceedings of Geo-Congress 2013: Stability and Performance of Slopes and Embankments III, San Diego, CA, March 3–7, ASCE, Reston, VA, 2013, pp. 413–416, https://doi.org/10.1061/9780784412787.041.
- [16] N.W. Facas, R.V. Rinehart, M.A. Mooney, Development and evaluation of relative compaction specifications using roller-based measurements, Geotech. Test. J. 34 (6) (2011) 634–642. https://doi.org/10.1520/GTJ102915.
- [17] N.W. Facas, M.A. Mooney, Position reporting error of intelligent compaction and continuous compaction control roller-measured soil properties, J. Test. Eval. 38 (1) (2009) 13–18, https://doi.org/10.1520/JTE102323.
- [18] C.L. Meehan, D.V. Cacciola, F.S. Tehrani, W.J. Baker III, Assessing soil compaction using continuous compaction control and location-specific in situ tests, Autom. Constr. 73 (2017) 31–44, https://doi.org/10.1016/j.autcon.2016.08.017.
- [19] M.J. Thompson, D.J. White, Estimating compaction of cohesive soils from machine drive power, J. Geotech. Geoenviron. 134 (12) (2008) 1771–1777, https://doi.org/ 10.1061/(ASCF)1090-0241(2008)134:12(1771.
- [20] D.H. Liu, Z.L. Li, Z.H. Lian, Compaction quality assessment of earth-rock dam materials using roller-integrated compaction monitoring technology, Autom. Constr. 44 (2014) 234–246, https://doi.org/10.1016/j.autcon.2014.04.016.
- [21] P.K.R. Vennapusa, D.J. White, M.D. Morris, Geostatistical analysis for spatially referenced roller-integrated compaction measurements, J. Geotech. Geoenviron. 136 (6) (2010) 813–822, https://doi.org/10.1061/(ASCE)GT.1943-5606.0000285.
- [22] D.J. White, E.J. Jaselskis, V.R. Schaefer, E.T. Cackler, Real-time compaction monitoring in cohesive soils from machine response, Transp. Res. Rec. 1936 (2005) 73–180, https://doi.org/10.1177/0361198105193600120.
- [23] P.K.R. Vennapusa, D.J. White, S. Schram, Roller-integrated compaction monitoring for hot-mix asphalt overlay construction, J. Transp. Eng. 139 (12) (2013) 1164–1173, https://doi.org/10.1061/(ASCE)TE.1943-5436.0000602.
- [24] P.K.R. Vennapusa, D.J. White, Machine drive power based roller-integrated compaction measurements for cohesive embankment construction, Geo-Chicago 2016 (2016) 571–580, https://doi.org/10.1061/9780784480151.056.
- [25] R. Rinehart, M. Mooney, N. Facas, O. Musimbi, Examination of roller-integrated continuous compaction control on Colorado test site, Transp. Res. Rec. 2310 (2012) 3–9, https://doi.org/10.3141/2310-01 (Transportation Research Board of the National Academies, Washington, D.C., USA).
- [26] P.K.R. Vennapusa, D.J. White, J. Siekmeier, R.A. Embacher, In situ mechanistic characterizations of granular pavement foundation layers, Int. J. Pavement Eng. 13 (1) (2012) 52–67, https://doi.org/10.1080/10298436.2011.564281.
- [27] D.J. White, M.J. Thompson, Relationships between in situ and roller-integrated compaction measurements for granular soils, J. Geotech. Geoenviron. 134 (12) (2008) 1763–1770, https://doi.org/10.1061/(ASCE)1090-0241(2008) 134:12(1763).
- [28] Å. Sandström, C.B. Pettersson, Intelligent systems for QA/QC in soil compaction, Proceedings of the Annual Transportation Research Board Meeting, Transportation Research Board, Washington, D.C., USA, 03-0909-461-5, 2004.
- [29] D.J. White, M.J. Thompson, P. Vennapusa, Field Validation of Intelligent Compaction Monitoring Technology for Unbound Materials, Final Report, Minnesota Department of Transportation, Maplewood, Minnesota, USA, 2007https://lib.dr.iastate.edu/cgi/viewcontent.cgi?article = 1001&context = intrans_techtransfer.
- [30] G. Komandi, An evaluation of the concept of rolling resistance, J. Terrramech. 36

- (3) (1999) 159-166, https://doi.org/10.1016/S0022-4898(99)00005-1.
- [31] M. Mooney, D. Adam, Vibratory roller integrated measurement of earthwork compaction: an overview, Seventh International Symposium on Field Measurements in Geomechanics, ASCE, 2007, https://doi.org/10.1061/40940(307)80.
- [32] D.H. Zhong, D.H. Liu, B. Cui, Real-time compaction quality monitoring of high core rockfill dam, SCIENCE CHINA Technol. Sci. 54 (7) (2011) 1906–1913, https://doi. org/10.1007/s11431-011-4429-6.
- [33] Q.L. Zhang, T.Y. Liu, Q.B. Li, Roller-integrated acoustic wave detection technique for rockfill materials, Appl. Sci. 7 (2017) 1118, https://doi.org/10.3390/ app7111118.
- [34] J. Scherocman, S. Rakowski, K. Uchiyama, Intelligent compaction, does it exist? 2007 Canadian Technical Asphalt Association (CTAA) Conference, Victoria, BC, 2007, pp. 1–25 http://www.intelligentcompaction.com/downloads/ PapersReports/Saikai_Jim%20Sherocman_IC%20Does%20it%20Exist_CTAA_2007. pdf.
- [35] M.A. Mooney, R.V. Rinehart, N.W. Facas, O.M. Musimbi, D.J. White, P. Vennapusa, Intelligent soil compaction systems, Final Report, NCHRP 676, Transportation Research Board, Washington, D.C., 978-0-309-15519-9, 2010.
- [36] S. Commuri, A.T. Mai, M. Zaman, Neural network-based intelligent compaction analyzer for estimating compaction quality of hot asphalt mixes, J. Constr. Eng. Manag. 137 (9) (2011) 633–715, https://doi.org/10.1061/(ASCE)CO.1943-7862. 0000343
- [37] F. Beainy, S. Commuri, M. Zaman, Quality assurance of hot mix asphalt pavements using the intelligent asphalt compaction analyzer, J. Constr. Eng. Manag. 138 (2) (2012) 178–187, https://doi.org/10.1061/(ASCE)CO.1943-7862.0000420.
- [38] Q.W. Xu, G.K. Chang, Evaluation of intelligent compaction for asphalt materials, Autom. Constr. 30 (2013) 104–112, https://doi.org/10.1016/j.autcon.2012.11.
- [39] Q.W. Xu, G.K. Chang, Experimental and numerical study of asphalt material geospatial heterogeneity with intelligent compaction technology on roads, Constr. Build. Mater. 72 (2014) 189–198, https://doi.org/10.1016/j.conbuildmat.2014.09.
- [40] W. Hu, X. Shu, X.Y. Jia, B.S. Huang, Recommendations on intelligent compaction parameters for asphalt resurfacing quality evaluation, J. Constr. Eng. Manag. 143 (9) (2017) 04017065, https://doi.org/10.1061/(ASCE)CO.1943-7862.0001361.
 [41] S.J. Yoon, M. Hastak, J.S. Lee, Suitability of intelligent compaction for asphalt
- [41] S.J. Yoon, M. Hastak, J.S. Lee, Suitability of intelligent compaction for asphalt pavement quality control and quality assurance, J. Constr. Eng. Manag. 144 (4) (2018) 04018006, https://doi.org/10.1061/(ASCE)CO.1943-7862.0001401.
- [42] Q.W. Xu, G.K. Chang, Adaptive quality control and acceptance of pavement material density for intelligent road construction, Autom. Constr. 62 (2016) 78–88, https://doi.org/10.1016/j.autcon.2015.11.004.
- [43] Q.W. Xu, G.K. Chang, V.L. Gallivan, Development of a systematic method for intelligent compaction data analysis and management, Constr. Build. Mater. 37 (2012) 470–480. https://doi.org/10.1016/j.conbuildmat.2012.08.001.
- [44] Q.W. Xu, G.K. Chang, V.L. Gallivan, R.D. Horan, Influences of intelligent compaction uniformity on pavement performances of hot mix asphalt, Constr. Build. Mater. 30 (2012) 746–752, https://doi.org/10.1016/j.conbuildmat.2011.12.082.
- 30 (2012) 746–752, https://doi.org/10.1016/j.conbuildmat.2011.12.082.
 [45] R.E. Minchin, D.C. Swanson, A.F. Gruss, H.R. Thomas, Computer applications in intelligent compaction, J. Comput. Civ. Eng. 22 (2008) 243–251, https://doi.org/10.1061/(ASCE)0887-3801(2008)22:4(243).
- [46] M. Barman, M. Nazari, S.A. Imran, S. Commuri, M. Zaman, F. Beainy, D. Singh, Quality control of subgrade soil using intelligent compaction, Innov. Infrastruct. Solut. 1 (2) (2016) 1–14, https://doi.org/10.1007/s41062-016-0020-0.
- [47] H.B. Cai, T. Kuczek, P.S. Dunston, S. Li, Correlating intelligent compaction data to in situ soil compaction quality measurements, J. Constr. Eng. Manag. 143 (8) (2017) 04017038, https://doi.org/10.1061/(ASCE)CO.1943-7862.0001333.
- [48] X.Y. Zhu, S.J. Bai, G.P. Xue, J. Yang, Y.S. Cai, W. Hu, X.Y. Jia, B.S. Huang, Assessment of compaction quality of multi-layer pavement structure based on intelligent compaction technology, Constr. Build. Mater. 161 (2018) 316–329, https://doi.org/10.1016/j.conbuildmat.2017.11.139.
- [49] S.A. Imran, M. Barman, S. Commuri, M. Zaman, M. Nazari, Artificial neural net-work-based intelligent compaction analyzer for real-time estimation of subgrade quality, Int. J. Geomech. 18 (6) (2018) 04018048, https://doi.org/10.1061/(ASCE)GM.1943-5622.0001089.
- [50] S.K. Kim, J. Seo, J.S. Russell, Intelligent navigation strategies for an automated earthwork system, Autom. Constr. 21 (2012) 132–147, https://doi.org/10.1016/j. autcon.2011.05.021.
- [51] S.K. Kim, J.S. Russell, Framework for an intelligent earthwork system: part I. System architecture, Autom. Constr. 12 (2003) 1–13, https://doi.org/10.1016/

- S0926-5805(02)00034-1.
- [52] R.V. Rinehart, M.A. Mooney, Instrumentation of a roller compactor to monitor vibration behavior during earthwork compaction, Autom. Constr. 17 (2008) 144–150, https://doi.org/10.1016/j.autcon.2006.12.006.
- [53] Y. Ju, G. Lin, Y. Fan, Z. Liu, Intelligent compaction control based on fuzzy neural network, Sixth International Conference on Parallel and Distributed Computing Applications and Technologies (PDCAT'05), IEEE Computer Society, Dalian, China, 2005, https://doi.org/10.1109/PDCAT.2005.156.
- [54] X.W. Luo, Z.G. Zhang, Z.X. Zhao, B. Chen, L. Hu, X.P. Wu, Design of DGPS navigation control system for Dongfanghong X-804 tractor, Trans. Chin. Soc. Agric. Eng. 25 (11) (2009) 139–144, https://doi.org/10.3969/j.issn.1002-6819.2009.11.025.
- [55] L.G. Wei, Q. Zhang, H. Yan, Y.C. Liu, GPS automatic navigation system design for XDNZ630 rice transplanter, Trans. Chin. Soc. Agric. Mach. 42 (7) (2011) 186–190, https://doi.org/10.3969/j.issn.1000-1298.2011.07.035.
- [56] E. Kassem, W.T. Liu, T. Scullion, E. Masad, A. Chowdhury, Development of compaction monitoring system for asphalt pavements, Constr. Build. Mater. 96 (2015) 334–345, https://doi.org/10.1016/j.conbuildmat.2015.07.041.
- [57] R. Anderegg, D.A. von Felten, K. Kaufmann, Compaction monitoring using intelligent soil compactors, GeoCongress 2006: Geotechnical Engineering in the Information Technology Age, Atlanta, 2006, https://doi.org/10.1061/40803(187)41
- [58] D.V. Cacciola, Using continuous compaction control systems within an earthwork compaction specification framework, A Thesis Submitted to the Faculty of the University of Delaware in Partial Fulfillment of the Requirements for the Degree of Master of Civil Engineering, 2013 http://dspace.udel.edu/bitstream/handle/19716/12878/Daniel Cacciola thesis.pdf?sequence=1&isAllowed=y.
- [59] D.V. Cacciola, M. Khosravi, C.L. Meehan, Using compaction equipment instrumented with global positioning system (GPS) technology to monitor field lift thickness, GeoCongress 2014: Geo-characterization and Modeling for Sustainability, Geotechnical Special Publication No. 234, ASCE, Reston, VA, 2014, pp. 2630–2639. https://doi.org/10.1061/9780784413272.254.
- [60] C.L. Meehan, M. Khosravi, D.V. Cacciola, Monitoring field lift thickness using compaction equipment instrumented with global positioning system (GPS) technology, Geotech. Test. J. 36 (5) (2013) 755–767, https://doi.org/10.1520/ CT120120124
- [61] E.H. Isaaks, R.M. Srivastava, An Introduction to Applied Geostatistics, Oxford University Press, New York, 01-9505-012-6, 1989.
- [62] M.J. Thompson, D.J. White, Field calibration and spatial analysis of compaction monitoring technology measurements, Transp. Res. Rec. 2004 (1) (2007) 69–79, https://doi.org/10.3141/2004-08.
- [63] K. Kaufmann, R. Anderegg, 3D-Construction application III GPS-based compaction technology, 1st International Conference on Machine Control & Guidance, ETH Zurich, Switzerland, 2008, pp. 1–10 https://pdfs.semanticscholar.org/4366/ 3295f28a737edf1ba9f18f5e594d2b8bd706.ndf.
- [64] P.T. Corcoran, F. Fernandez, Method and apparatus for determining the performance of a compaction machine based on energy transfer, United States Patent: US 6188942, 2001, http://www.freepatentsonline.com/6188942.pdf.
- [65] Trimble Company Website, https://www.trimble.com/, (2018).
- [66] T.Y. Liu, Q.B. Li, K. Fang, Vibratory roller automatic driving system and method for hydraulic engineering, China Patent: 201510609822. 2015, http://egaz.sipo.gov. cn/FileWeb/pfs?path = _ xCyNkckhqhGFwjTAa40bDPQVbfvNFVxO0ZNpM2k7doqtG46qFLiGirHZFKw4 xUFsQ86JdxsHMH6gxow8dxu4wU3_L5li6yjR8n9Ga9fT-k.
- [67] Q.L. Zhang, T.Y. Liu, Q.B. Li, Z.Z. An, L. Fan, Automatic rolling system based on closed-loop feedback control and RTK-GPS, J. Hydroelectr. Eng. 37 (5) (2018) 151–160 http://manul3.magtech.com.cn/slfdxb/CN/10.11660/slfdxb.20180516.
- [68] J.G. Shi, C.X. Liu, H.Q. Xi, Improved D* path planning algorithm based on CA model, J. Electron. Meas. Instrum. 30 (1) (2016) 30–37 http://dx.chinadoi.cn/10.13382/j.jemi.2016.01.004.
- [69] X. Su, S. Li, C.X. Yuan, H.B. Cai, V.R. Kamat, Enhanced boundary condition-based approach for construction location sensing using RFID and RTK GPS, J. Constr. Eng. Manag. 140 (10) (2014) 04014048, https://doi.org/10.1061/(ASCE)CO.1943-7862.0000889.
- [70] G.W. Robert, A.H. Dodson, V. Ashkenazi, Global position system aided autonomous construction plant control and guidance, Autom. Constr. 8 (5) (1999) 589–595, https://doi.org/10.1016/S0926-5805(99)00008-4.
- [71] D.H. Liu, M. Lin, S. Li, Real-time quality monitoring and control of highway compaction, Autom. Constr. 62 (2016) 114–123, https://doi.org/10.1016/j.autcon. 2015.11.007.